Direct Determination of Exchange Parameters in Cs_2CuBr_4 and Cs_2CuCl_4: High-Field Electron-Spin-Resonance Studies

S. A. Zvyagin,[1] D. Kamenskyi,[1,*] M. Ozerov,[1] J. Wosnitza,[1,2] M. Ikeda,[3] T. Fujita,[3] M. Hagiwara,[3] A. I. Smirnov,[4] T. A. Soldatov,[5] A. Ya. Shapiro,[6] J. Krzystek,[7] R. Hu,[8,†] H. Ryu,[8,9] C. Petrovic,[8,9] and M. E. Zhitomirsky[10]

[1]*Dresden High Magnetic Field Laboratory (HLD), Helmholtz-Zentrum Dresden-Rossendorf, 01328 Dresden, Germany*
[2]*Institüt fur Festkörperphysik, TU Dresden, 01068 Dresden, Germany*
[3]*KYOKUGEN, Osaka University, Toyonaka, Osaka 560-8531, Japan*
[4]*P.L. Kapitza Institute for Physical Problems, RAS, 119334 Moscow, Russia*
[5]*Moscow Institute for Physics and Technology, 141700 Dolgoprudnyi, Russia*
[6]*A.V. Shubnikov Institute of Crystallography, RAS, 119333, Moscow, Russia*
[7]*National High Magnetic Field Laboratory, Florida State University, Tallahassee, Florida 32310, USA*
[8]*Condensed Matter Physics and Materials Science Department, Brookhaven National Laboratory, Upton, New York 11973, USA*
[9]*Department of Physics and Astronomy, Stony Brook University, Stony Brook, New York 11794-3800, USA*
[10]*Service de Physique Statistique, Magnétisme et Supraconductivité, UMR-E9001 CEA-INAC/UJF, 38054 Grenoble Cedex 9, France*

(Received 12 December 2013; revised manuscript received 23 January 2014; published 20 February 2014)

Spin-1/2 Heisenberg antiferromagnets Cs_2CuCl_4 and Cs_2CuBr_4 with distorted triangular-lattice structures are studied by means of electron spin resonance spectroscopy in magnetic fields up to the saturation field and above. In the magnetically saturated phase, quantum fluctuations are fully suppressed, and the spin dynamics is defined by ordinary magnons. This allows us to accurately describe the magnetic excitation spectra in both materials and, using the harmonic spin-wave theory, to determine their exchange parameters. The viability of the proposed method was proven by applying it to Cs_2CuCl_4, yielding $J/k_B = 4.7(2)$ K, $J'/k_B = 1.42(7)$ K, $[J'/J \simeq 0.30]$ and revealing good agreement with inelastic neutron-scattering results. For the isostructural Cs_2CuBr_4, we obtain $J/k_B = 14.9(7)$ K, $J'/k_B = 6.1(3)$ K, $[J'/J \simeq 0.41]$, providing exact and conclusive information on the exchange couplings in this frustrated spin system.

DOI: 10.1103/PhysRevLett.112.077206 PACS numbers: 75.40.Gb, 75.10.Jm, 75.50.Ee, 76.30.-v

A spin-1/2 Heisenberg antiferromagnet (AF) on a triangular lattice is the paradigmatic model in quantum magnetism, which has been intensively studied since Anderson's conjecture of the resonating-valence-bond ground state [1]. In spite of numerous theoretical studies (which predict a rich variety of grounds states, ranging from a gapless spin liquid to Néel order), many important details of the phase diagram of triangular-lattice AFs remain controversial or even missing (see, i.e., [2–7]).

In order to test the theory experimentally, a precise information on the spin-Hamiltonian parameters for the materials of interest is highly demanded. The presence of quantum fluctuations makes the accurate description of such systems (first of all, the extraction of the spin Hamiltonian parameters) extremely challenging. One solution for solving this problem is to suppress quantum fluctuations by strong-enough magnetic fields. The system is then in the spin-polarized, magnetically saturated phase. The excitation spectrum above the saturation field, $H_{\rm sat}$, is determined by ordinary magnons, which can be described quantitatively by a simple harmonic spin-wave theory.

Studying the magnon dispersion in quantum magnets above $H_{\rm sat}$ by means of inelastic neutron-scattering provides the most straightforward opportunity for extracting parameters of the spin Hamiltonian. This method has been used, for instance, to determine the exchange coupling parameters in the triangular-lattice AF Cs_2CuCl_4 [8]. Experiments revealed up to 65% difference between the parameters estimated at $H = 0$ (using the harmonic approximation) and actual values (extracted from measurements at $H > H_{\rm sat}$), stressing the great importance of high-field experiments. Unfortunately, the applicability of this technique is limited to magnetic fields (of about 15 T) currently available for neutron-scattering experiments.

Electron spin resonance (ESR) offers another means for measuring the spin Hamiltonian parameters, directly and with high precision. Similar to the case of neutron scattering, the distinct advantage of the high-field ESR is the availability of *exact* theoretical spin-wave expressions for the magnetically saturated phase. For instance, measurements of ESR spectra in the spin-1 material $NiCl_2$-4SC$(NH_2)_2$ (known as DTN) above the saturation field, $H_{\rm sat} = 12.6$ T, allowed us to determine the bare single-ion anisotropy and, based on that, to accurately describe the temperature-field phase diagram [9].

In this Letter, we report on a new approach, which combines high-field ESR as a tool to probe the magnon-excitation spectrum above H_{sat} and its classical linear spin-wave description, allowing us to accurately determine exchange coupling parameters in a spin-1/2 Heisenberg triangular-lattice AF. This approach is based on the observation of ESR modes of a new type, which become possible due to the low-enough crystal symmetry of the studied materials. First, we proved the viability of the proposed technique by applying it to Cs_2CuCl_4. Good agreement between the neutron-scattering [8] and ESR results was obtained. Then, this procedure was employed for the determination of the exchange parameters in the isostructural compound Cs_2CuBr_4, providing the direct answer to the long-standing problem of the spin Hamiltonian parameters of this frustrated compound.

In spite of the recent progress in synthesizing new spin-1/2 triangular-lattice materials (see [10–14] and references herein) the two compounds, Cs_2CuCl_4 and Cs_2CuBr_4 (hereafter called CCC and CCB), remain among the most prominent representatives of such kinds of frustrated magnets. The Cu^{2+} ions in CCC and CCB form a distorted triangular lattice and can be described by the exchange Hamiltonian

$$\mathcal{H} = J\sum_{\langle i,j\rangle} \mathbf{S}_i \cdot \mathbf{S}_j + J'\sum_{\langle i,j'\rangle} \mathbf{S}_i \cdot \mathbf{S}_{j'}, \qquad (1)$$

where $\mathbf{S}_i$, $\mathbf{S}_j$, and $\mathbf{S}_{j'}$ are spin-1/2 operators at sites i, j, and j', respectively; J is the interaction constant along the b direction; J' is the zigzag interchain coupling [Fig. 1(a)]. The orthorhombic crystal structure of CCC corresponds to the space group *Pnma* with the room-temperature lattice parameters $a = 9.769$ Å, $b = 7.607$ Å, and $c = 12.381$ Å [15]. At $T_N = 0.62$ K, CCC undergoes a transition into a helical incommensurate (IC) long-range-ordered state [16]. CCC is in the saturated phase above the critical fields $H_{sat} = 8.44$, 8.89, and 8 T applied along the a, b, and c axes, respectively

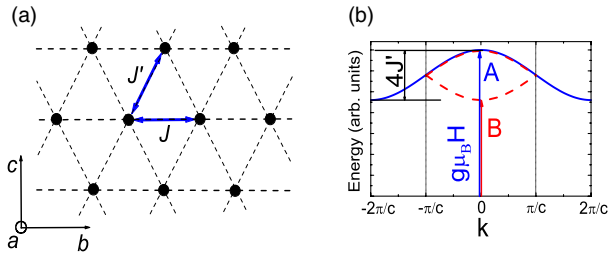

FIG. 1 (color online). (a) Schematic picture of exchange paths in the bc plane of CCC and CCB. (b) Dispersion of magnon excitations for a spin-1/2 Heisenberg AF with triangular lattice in the saturated phase for an arbitrary magnetic field. Solid blue line is the dispersion of magnon excitations in the exchange approximation (Eq. 4). The magnon dispersion within the folded Brillouin zone is shown by the dashed red line. Arrows A and B correspond to the observed ESR transitions.

[17]. The exchange interactions were estimated from the inelastic neutron-scattering experiments in the saturated phase mentioned above [8], yielding $J/k_B = 4.34(6)$ K and $J'/k_B = 1.48(6)$ K [$J'/J = 0.34(2)$].

Similar to CCC, the isostructural compound CCB realizes a distorted triangular lattice with the room-temperature lattice parameters $a = 10.195$ Å, $b = 7.965$ Å, and $c = 12.936$ Å [18]. At $T_N = 1.4$ K, CCB undergoes a transition into the helical IC long-range-ordered state [19,20]. CCB is in the saturated phase above $H_{sat} = 30.71$, 30.81, and 28.75 T applied along the a, b, and c axes, respectively [21]. Within a classical spin model, the ratio $J'/J = 0.467$ was estimated [19–21]. On the other hand, results of density-functional calculations suggest $J'/J \sim 0.5$–0.65 [22], while the ratio $J'/J = 0.74$ was obtained [23] by comparison of the zero-field IC wave number in the ordered phase with results of the series expansion method [24].

Single crystals of CCC (CCB) were synthesized by slow evaporation of aqueous solutions of CsCl and $CuCl_2$ (CsBr and $CuBr_2$). Samples of CCC were from the same batch as in Refs. [25,26]. Experiments were performed using ESR spectrometers operated in combination with superconducting (KYOKUGEN, HLD, Kapitza Institute), 25 T resistive (NHMFL [27]), and 50 T pulse-field (KYOKUGEN, HLD) magnets. The spectrometer at the Kapitza Institute with a ^{3}He insert and 12 T magnet was used for taking spectra down to 0.45 K. Backward wave oscillators, VDI generators (product of Virginia Diodes Inc.), and a CO_2-pumped molecular laser (product of Edinburgh Instruments Ltd.) were used as sources of mm- and submm-wavelength radiation. In our experiments, the magnetic field was applied along the crystallographic b axis. 2,2-diphenyl-1-picrylhydrazyl (known as DPPH) was employed as a standard marker for the accurate calibration of the magnetic field.

The frequency-field diagrams of the ESR absorption in CCC at 0.5 and 1.5 K are shown in Fig. 2 by squares and circles, respectively. Two resonance modes of different intensity were observed [Fig. 3(a)]. The most intensive mode, mode A, can be described using the equation $\hbar\omega_A = \sqrt{(g_b\mu_B H)^2 + \Delta_A^2}$, where $\hbar$ is the Planck constant, ω is the excitation frequency, μ_B is the Bohr magneton, $\Delta_A/(2\pi\hbar) = 14$ GHz and $g_b = 2.08(2)$ [25]. Above H_{sat}, mode A corresponds to the collective excitation of spins with the frequency $\omega_A \approx g_b\mu_B H/\hbar$ and can be interpreted as uniform $\mathbf{k} = 0$ precession of spins around the field direction. The much weaker mode B appears at $H \gtrsim H_{sat}$. The frequency of this mode can be described empirically using the equation $\hbar\omega_B = g_b\mu_B H - \Delta_B$ with the same g factor, $g_b = 2.08$, and $\Delta_B/(2\pi\hbar) = 119.0(3)$ GHz. The ESR line undergoes a significant broadening approaching H_{sat} from the high-field end (Fig. 2, triangles), becoming undetectable below 8 T. An example of ESR spectrum (mode B), taken at 178.3 GHz ($T = 0.53$ K) is shown in the inset of Fig. 2; the solid line corresponds to a Lorentzian fit.

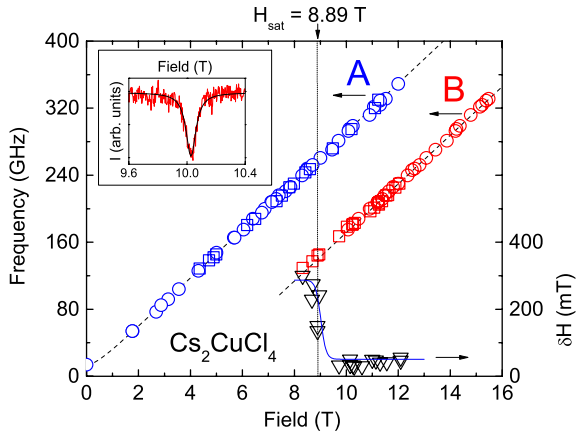

FIG. 2 (color online). Frequency-field diagram of the ESR excitations in CCC measured at 0.5 K (squares) and 1.5 K (circles). Dashed lines correspond to fit results (see text for details). The linewidth (half width at half maximum) of mode B vs field is shown by triangles; the solid line is a guide for the eye. Inset shows an example of ESR spectrum (mode B) taken at 178.3 GHz ($T = 0.53$ K); the solid line corresponds to a Lorentzian fit.

The emergence of two ESR modes in the magnetically saturated state signifies a lower crystal symmetry compared to the one assumed in the simple spin model (1). This is not entirely surprising since the unit cell of CCC is made up of four inequivalent Cu^{2+} ions: two on the adjacent b chains in the bc plane and two on the adjacent layer shifted along the b and c axes by a half of the lattice constant [16]. One single copper layer is described by the exchange Hamiltonian (1). On the other hand, the crystal symmetry of CCC allows the Dzyaloshinskii-Moriya (DM) interaction for all nearest-neighbor spin bonds in a single copper layer

$$\hat{\mathcal{H}}_{\mathrm{DM}} = \sum_i \sum_{n=1}^{3} \mathbf{D}_n \cdot [\mathbf{S}_i \times \mathbf{S}_{i+\boldsymbol{\delta}_n}], \tag{2}$$

where the lattice vectors $\boldsymbol{\delta}_n$ are chosen as $\boldsymbol{\delta}_1 = (0, b, 0)$, $\boldsymbol{\delta}_{2,3} = (0, \pm b/2, c/2)$. The DM vectors compatible with the space group of the crystal are given by

$$\begin{aligned} \mathbf{D}_1 &= [D_a, 0, (-1)^{i_c} D_c], \\ \mathbf{D}_{2,3} &= [\pm D_a', (-1)^{i_c} D_b', \pm(-1)^{i_c} D_c'], \end{aligned} \tag{3}$$

where i_c is the chain index in the c direction (see [5] for further details on the DM interactions in CCC). So far, experiments on CCC gave estimates for three DM parameters: $D_a'/J \sim 5\%$ [8] and $D_{a,c}/J \sim 10\%$ [25,28].

The reduced translational symmetry of the copper layers in CCC (CCB) revealed by the staggered DM vectors (3) leads to the folding of the Brillouin zone of a simple triangular Bravais lattice. As a result, the ESR transitions are allowed not only for $\mathbf{k} = 0$ (mode A) but also for $k_c = 2\pi/c$ (exchange mode B). A detailed analysis of the excitation spectrum for the spin Hamiltonian given by the sum of (1) and (2) is presented in the Supplemental Material [29]. Here, we resort to a simpler line of arguments valid in the case of small DM interaction. We just neglect the effect of the DM terms (2) on the magnon energy. Then, the dispersion of the magnetic excitations for a spin-1/2 AF (1) in the saturated phase is described by

$$\begin{aligned} \hbar\omega_{\mathbf{k}} &= g\mu_B H + J\cos(k_b b) \\ &\quad + 2J'\cos\left(\frac{1}{2}k_b b\right)\cos\left(\frac{1}{2}k_c c\right) - J_0, \end{aligned} \tag{4}$$

where $J_0 = J + 2J'$. The difference between the excitation energies of the modes A and B [Fig. 1(b)] is equal to

$$\hbar\Delta\omega = 4J'. \tag{5}$$

For $\mathbf{H}\|b$, the above approximate expression can be compared to the exact result [29]

$$\hbar\Delta\omega = 4\sqrt{(J')^2 + (D_b')^2}. \tag{6}$$

For this, as well as for other field orientations, the correction from a finite value of the DM interaction is of the order of $(D_b'/J')^2$ and does not exceed 1%–2%. However, a finite value of D_b' is essential for the observation of mode B: the intensity ratio of the two resonance lines scales as $(D_b'/J')^2$, so that mode B would not be seen for $D_b' = 0$. Hence, measurements of the ESR spectra in the saturated phase provide a direct and accurate estimate of J'.

Knowing J', we now can determine J from the saturation field using the expression

$$g\mu_B H_{\mathrm{sat}} = 2J(1 + J'/2J)^2 \tag{7}$$

obtained for the exchange model (1). The correction to Eq. (7), taking the DM interactions into account, can be assessed using the expression obtained for $\mathbf{H}\|b$ [29]

$$g\mu_B H^b_{\mathrm{sat}} = 2(J + J') + (J'^2 + D_b'^2)/2J. \tag{8}$$

Even for $D_b' \sim 0.1$–$0.2J$, the effect on H_{sat} for CCC(CCB) can be safely neglected. Thus, using Eqs. (4) and (7), $g_b = 2.08(2)$, and $H_{\mathrm{sat}} = 8.89(2)$ T, the exchange coupling parameters for CCC are obtained as $J/k_B = 4.7(2)$ K and $J'/k_B = 1.42(7)$ K [$J'/J = 0.30(3)$] [30]. The latter value is in good agreement with the estimate $J'/J = 0.34(2)$ from the neutron-scattering experiments [8].

Let us also note that, in CCC (CCB), the Brillouin-zone folding occurs also in the a direction perpendicular to the copper layers. By a similar line of arguments, this folding yields a further splitting of each mode A and B by $\delta\omega'' \sim J''$, where J'' is the interlayer exchange coupling. Since $J' = 0.2$ K [8], it is rather difficult to observe such a splitting even in ESR experiments.

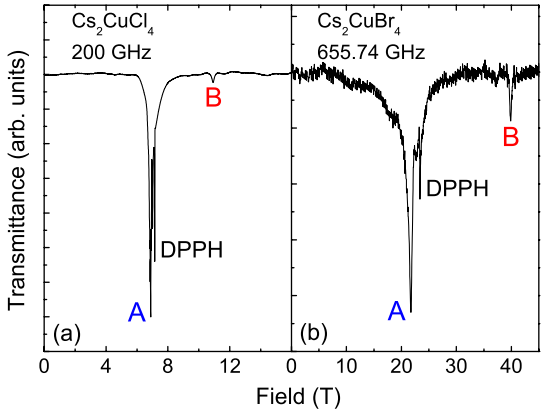

FIG. 3 (color online). ESR spectra of CCC (a) and CCB (b), taken at frequencies 200 and 655.74 GHz, respectively ($T = 1.5$ K). DPPH is employed as a standard marker.

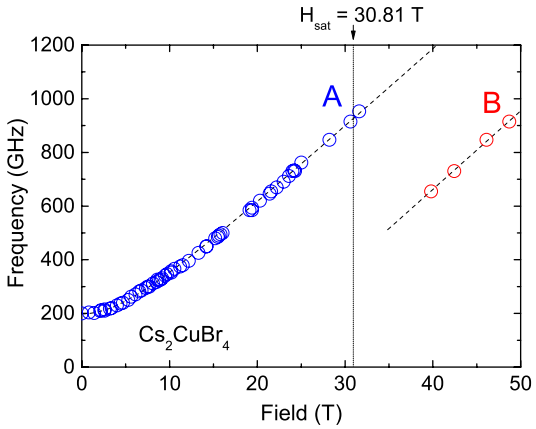

FIG. 4 (color online). Frequency-field diagram of ESR excitations in CCB ($T = 1.5$ K). Dashed lines correspond to fit results (see the text for details).

Once the viability of the proposed approach is verified, we apply it now to CCB. Compared to CCC, $H_{\rm sat}$ in CCB is more than 3 times larger, that implies the necessity of ESR measurements in magnetic field above 30 T. Similar to CCC, two ESR modes have been observed at $H > H_{\rm sat}$ [Fig. 3(b)]. The frequency-field diagram of ESR excitations in CCB obtained at $T = 1.5$ K is shown in Fig. 4. Mode A can be described using the equation $\hbar\omega_A = \sqrt{(g\mu_B H)^2 + \Delta_A^2}$, where $g_b = 2.09(2)$ and $\Delta_A/(2\pi\hbar) = 198$ GHz. Exchange mode B was observed only above $H_{\rm sat}$. Mode B can be described by the equation $\hbar\omega_B = g_b\mu_B H - \Delta_B$, where $\Delta_B/(2\pi\hbar) = 507.6$ GHz. Using Eqs. (4) and (7), the exchange coupling parameters for CCB are obtained: $J/k_B = 14.9(7)$ K and $J'/k_B = 6.1(3)$ K [$J'/J = 0.41(4)$] [30].

As mentioned, our results for CCC are in a good agreement with those obtained earlier using inelastic neutron-scattering experiments [8]. On the other hand, in the case of CCB, a relatively big difference between the previously suggested value, $J'/J = 0.74$ [21], and our result, $J'/J = 0.41(4)$, is observed. This difference is of crucial importance for understanding the unusual magnetic properties of CCB. For instance, CCB is a rare example of a spin-1/2 triangular-lattice Heisenberg AF, which exhibits a 1/3 magnetization plateau [19–21]. Numerical diagonalization calculations of a finite-size spin-1/2 Heisenberg AF predicts that the geometric frustration should be sufficiently strong to stabilize the so-called "up-up-down" (UUD) phase, resulting in the emergence of the 1/3 magnetization plateau, in the range $0.7 \lesssim J'/J \lesssim 1.3$ [31]. On the other hand, density matrix renormalization group calculations predict the 1/3 magnetization plateau even for an infinitesimally small J'/J ratio [32]. Our results suggest that the field-induced "up-up-down" phase in spin-1/2 triangle-lattice Heisenberg AFs can be realized for the J'/J ratio, which is much smaller than predicted in Ref. [31]. The obtained spin-Hamiltonian parameters can be of particular importance for a quantitative description of the cascade of field-induced phase transitions observed recently in CCB [33].

In conclusion, the excitation spectra of Cs_2CuCl_4 and Cs_2CuBr_4 have been probed in magnetic fields up to $H_{\rm sat}$ and above. Based on the classical linear spin-wave description of the magnon excitation spectrum and high-field magnetization data, the exchange coupling parameters for both compounds were determined. The obtained accurate knowledge is of eminent importance for the understanding of the complex phase diagram of spin-1/2 triangular-lattice Heisenberg AFs. The proposed approach can be used for accurate estimation of exchange parameters of a growing family of spin-1/2 triangular-lattice AFs, including organic compounds (see [10–13] and references therein); those investigations via conventional neutron-scattering techniques are rather challenging. The employment of very high magnetic fields (up to ca 70 T [34,35] and above [36–38], currently available for pulsed-field magnetospectroscopy) as well as the rapid progress in the THz techniques makes the proposed method of crucial importance for investigating spin systems with large J/k_B. The approach has a broader impact and can be potentially used for any quantum magnet with reduced (e.g., by the staggered DM interaction) translational symmetry, resulting, as predicted, in emergence of a new exchange mode above $H_{\rm sat}$.

This work was supported in part by the DFG. We acknowledge the support of the HLD at HZDR, member of the European Magnetic Field Laboratory (EMFL). S. A. Z. appreciates the support of the Visiting Professor Program at KYOKUGEN in Osaka University. Work at Brookhaven was supported by the U.S. DOE under Contract No. DE-AC02-98CH10886. C. P. acknowledges the support by the A. von Humboldt Foundation. Work at the Kapitza Institute is supported by Russian Foundation for Basic Research, Grant No. 12-02-00557. A portion of this work was performed at the NHMFL, which is supported by NSF Cooperative Agreement No. DMR-1157490, by the State of

Florida, and by the U.S. DOE. The authors would like to thank V. N. Glazkov, A. K. Kolezhuk, V. I. Marchenko, S. S. Sosin, and O. A. Starykh for discussions, and S. Miyasaka for the help in orienting the CCB samples.

*Present address: Radboud University Nijmegen, Institute for Molecules and Materials, High Field Magnet Laboratory, 6500 GL Nijmegen, Netherlands

†Present address: Rutgers Center for Emergent Materials and Department of Physics and Astronomy, Rutgers University, Piscataway, NJ 08854, USA

[1] P. W. Anderson, Mater. Res. Bull. **8**, 153 (1973).
[2] M. Q. Weng, D. N. Sheng, Z. Y. Weng, and R. J. Bursill, Phys. Rev. B **74**, 012407 (2006).
[3] R. Schmied, T. Roscilde, V. Murg, D. Porras, and J. I. Cirac, New J. Phys. **10**, 045017 (2008).
[4] D. Heidarian, S. Sorella, and F. Becca, Phys. Rev. B **80**, 012404 (2009).
[5] O. A. Starykh, H. Katsura, and L. Balents, Phys. Rev. B **82**, 014421 (2010).
[6] S. Ghamari, C. Kallin, S. S. Lee, and E. S. Sørensen, Phys. Rev. B **84**, 174415 (2011).
[7] A. Weichselbaum and S. R. White, Phys. Rev. B **84**, 245130 (2011).
[8] R. Coldea, D. A. Tennant, K. Habicht, P. Smeibidl, C. Wolters, and Z. Tylczynski, Phys. Rev. Lett. **88**, 137203 (2002).
[9] S. A. Zvyagin, J. Wosnitza, C. D. Batista, M. Tsukamoto, N. Kawashima, J. Krzystek, V. S. Zapf, M. Jaime, N. F. Oliveira, and A. Paduan-Filho, Phys. Rev. Lett. **98**, 047205 (2007).
[10] M. Yamashita, N. Nakata, Y. Senshu, M. Nagata, H. M. Yamamoto, R. Kato, T. Shibauchi, and Y. Matsuda, Science **328**, 1246 (2010); T. Itou, A. Oyamada, S. Maegawa, and R. Kato, Nat. Phys. **6**, 673 (2010).
[11] S. Yamashita, Y. Nakazawa, M. Oguni, Y. Oshima, H. Nojiri, Y. Shimizu, K. Miyagawa, and K. Kanoda, Nat. Phys. **4**, 459 (2008); M. Yamashita, N. Nakata, Y. Kasahara, T. Sasaki, N. Yoneyama, N. Kobayashi, S. Fujimoto, T. Shibauchi, and Y. Matsuda, *ibid.* **5**, 44 (2008).
[12] K. Kanoda and R. Kato, Annu. Rev. Condens. Matter Phys. **2**, 167 (2011).
[13] B. J. Powell and R. H. McKenze, Rep. Prog. Phys. **74**, 056501 (2011).
[14] Y. Shirata, H. Tanaka, A. Matsuo, and K. Kindo, Phys. Rev. Lett. **108**, 057205 (2012); H. D. Zhou, C. Xu, A. M. Hallas, H. J. Silverstein, C. R. Wiebe, I. Umegaki, J. Q. Yan, T. P. Murphy, J.-H. Park, Y. Qiu, J. R. D. Copley, J. S. Gardner, and Y. Takano, *ibid.* **109**, 267206 (2012).
[15] S. Bailleul, D. Svoronos, P. Porchner, and A. Tomas, C.R. Acad. Sci. Ser. Gen., Ser. 2 **313**, 1149 (1991).
[16] R. Coldea, D. A. Tennant, R. A. Cowley, D. F. McMorrow, B. Dorner, and Z. Tylczynski, J. Phys. Condens. Matter **8**, 7473 (1996).
[17] Y. Tokiwa, T. Radu, R. Coldea, H. Wilhelm, Z. Tylczynski, and F. Steglich, Phys. Rev. B **73**, 134414 (2006).
[18] B. Morosin and E. C. Lingafelter, Acta Crystallogr. **13**, 807 (1960).
[19] T. Ono, H. Tanaka, O. Kolomiyets, H. Mitamura, T. Goto, K. Nakajima, A. Oosawa, Y. Koike, K. Kakurai, J. Klenke, P. Smeibidl, and M. Meissner, J. Phys. Condens. Matter **16**, S773 (2004).
[20] T. Ono, H. Tanaka, H. Aruga Katori, F. Ishikawa, H. Mitamura, and T. Goto, Phys. Rev. B **67**, 104431 (2003).
[21] T. Ono, H. Tanaka, O. Kolomiyets, H. Mitamura, F. Ishikawa, T. Goto, K. Nakajima, A. Oosawa, Y. Koike, K. Kakurai, J. Klenke, P. Smeibidl, M. Meissner, R. Coldea, A. D. Tennant, and J. Ollivier, Prog. Theor. Phys. Suppl. **159**, 217 (2005); T. Ono, H. Tanaka, T. Nakagomi, O. Kolomiyets, H. Mitamura, F. Ishikawa, T. Goto, K. Nakajima, A. Oosawa, Y. Koike, K. Kakurai, J. Klenke, P. Smeibidl, M. Meissner, and H. A. Katori, J. Phys. Soc. Jpn. **74**, 135 (2005).
[22] K. Foyevtsova, I. Opahle, Y.-Z. Zhang, H. O. Jeschke, and R. Valentí, Phys. Rev. B **83**, 125126 (2011).
[23] H. Tsujii, C. R. Rotundu, T. Ono, H. Tanaka, B. Andraka, K. Ingersent, and Y. Takano, Phys. Rev. B **76**, 060406(R) (2007).
[24] Zheng Weihong, R. H. McKenzie, and R. R. P. Singh, Phys. Rev. B **59**, 14367 (1999).
[25] K. Yu. Povarov, A. I. Smirnov, O. A. Starykh, S. V. Petrov, and A. Ya. Shapiro, Phys. Rev. Lett. **107**, 037204 (2011).
[26] A. I. Smirnov, K. Y. Povarov, S. V. Petrov, and A. Ya. Shapiro, Phys. Rev. B **85**, 184423 (2012).
[27] S. A. Zvyagin, J. Krzystek, P. H. M. van Loosdrecht, G. Dhalenne, and A. Revcolevschi, Physica (Amsterdam) **346–347B**, 1 (2004).
[28] M. A. Fayzullin, R. M. Eremina, M. V. Eremin, A. Dittl, N. van Well, F. Ritter, W. Assmus, J. Deisenhofer, H.-A. Krug von Nidda, and A. Loidl, Phys. Rev. B **88**, 174421 (2013).
[29] See Supplemental Material at http://link.aps.org/supplemental/10.1103/PhysRevLett.112.077206 for details of calculations.
[30] The largest error source in determining the exchange coupling parameters are the accuracy of the fit and the assumption of the DM contribution (which is less than 10%–15% of J). We estimate the accuracy of J and J' better than $\pm 5\%$.
[31] S. Miyahara, K. Ogino, and N. Furukawa, Physica (Amsterdam) **378–380B**, 587 (2006).
[32] R. Chen, H. Ju, H.-C. Jiang, O. A. Starykh, and L. Balents, Phys. Rev. B **87**, 165123 (2013).
[33] N. A. Fortune, S. T. Hannahs, Y. Yoshida, T. E. Sherline, T. Ono, H. Tanaka, and Y. Takano, Phys. Rev. Lett. **102**, 257201 (2009).
[34] S. A. Zvyagin, M. Ozerov, E. Čižmár, D. Kamenskyi, S. Zherlistyn, T. Herrmannsdörfer, J. Wosnitza, R. Wünsch, and W. Seidel, Rev. Sci. Instrum. **80**, 073102 (2009).
[35] S. A. Zvyagin, E. Čižmár, M. Ozerov, J. Wosnitza, R. Feyerherm, S. R. Manmana, and F. Mila, Phys. Rev. B **83**, 060409 (2011).
[36] H. Nojiri, Y. Shimamoto, N. Miura, M. Hase, K. Uchinokura, H. Kojima, I. Tanaka, and Y. Shibuya, Phys. Rev. B **57**, 10276 (1998).
[37] K. Kindo, S. Takeyama, M. Tokunaga, Y. H. Matsuda, E. Kojima, A. Matsuo, K. Kawaguchi, and H. Sawabe, J. Low Temp. Phys. **159**, 381 (2010).
[38] G. V. Boriskov, A. I. Bykov, M. I. Dolotenko, N. I. Egorov, Y. B. Kudasov, V. V. Platonov, V. D. Selemir, and O. M. Tatsenko, Phys. Usp. **54**, 421 (2011).